

# Femtosecond laser detection of Stark-decelerated and trapped methylfluoride molecules

Congsen Meng, Aernout P. P. van der Poel, Cunfeng Cheng, and Hendrick L. Bethlem

*LaserLaB, Department of Physics and Astronomy, VU University Amsterdam, De Boelelaan 1081, 1081 HV Amsterdam, Netherlands*

(Received 27 March 2015; published 7 August 2015)

We demonstrate deceleration and trapping of methylfluoride ( $\text{CH}_3\text{F}$ ) molecules in the low-field-seeking component of the  $J = 1, K = 1$  state using a combination of a conventional Stark decelerator and a traveling wave decelerator. The methylfluoride molecules are detected by nonresonant multiphoton ionization using a femtosecond laser. Subsequent mass and velocity selection of the produced ions enables us to eliminate most background signal resulting from thermal gas in our vacuum chamber. This detection method can be applied to virtually any molecule, thereby enhancing the scope of molecules that can be Stark decelerated. Methylfluoride is so far the heaviest and most complex molecule that has been decelerated to rest. Typically we trap  $2 \times 10^4$   $\text{CH}_3\text{F}$  molecules at a peak density of  $4.5 \times 10^7 \text{ cm}^{-3}$  and a temperature of 40 mK.

DOI: [10.1103/PhysRevA.92.023404](https://doi.org/10.1103/PhysRevA.92.023404)

PACS number(s): 37.10.Pq, 37.10.Mn, 37.20.+j

## I. INTRODUCTION

Cold molecules offer unique prospects for precision tests of fundamental physics theories, cold chemistry, and quantum computation (see, for instance, [1–4]). One of the techniques that has been successful in producing samples of cold and trapped molecules is Stark deceleration. This technique uses a series of electrodes at high voltage to generate an effective [5–7] or genuine [8–10] traveling potential well that moves along with molecules in a beam. By gradually lowering the velocity of the moving potential, molecules are decelerated and ultimately brought to a standstill. Stark deceleration has been applied to many molecules, including  $\text{CO}(a^3\Pi)$ ,  $\text{ND}_3$ ,  $\text{NH}_3$ ,  $\text{OH}$ ,  $\text{OD}$ ,  $\text{NH}(a^1\Delta)$ ,  $\text{H}_2\text{CO}$ ,  $\text{SO}_2$ ,  $\text{CaF}$ ,  $\text{YbF}$ ,  $\text{C}_7\text{H}_5\text{N}$ , and  $\text{SrF}$  [3]. So far (isotopomers of) four of these molecules,  $\text{NH}_3$ ,  $\text{OH}$ ,  $\text{CO}$ , and  $\text{NH}$ , have been brought to a standstill and subsequently confined in an electrostatic trap. For the success of Stark deceleration it is important that techniques are developed to increase the density and decrease the temperature of the trapped molecules, but also that the techniques become more general and can be applied to larger and heavier molecules. Here, we demonstrate deceleration and trapping of methylfluoride ( $\text{CH}_3\text{F}$ ) molecules, the largest and heaviest molecule that has been trapped using Stark deceleration so far. Methylfluoride is of interest for a number of reasons: (i) it is highly polarizable [11] and hence serves as a benchmark for studying steric effects in chemical reactions [12], (ii) it is a model system for ortho-para conversion [13], (iii) its structure makes it suitable for use in quantum computation and simulation schemes [14,15], and (iv) it can be further cooled by electrical-optical cooling [16]. Methylfluoride, as most polyatomic molecules, has no suitable transitions for detection via laser-induced fluorescence (LIF) or resonance-enhanced multiphoton ionization (REMPI) schemes that have been used in previous experiments on Stark deceleration. In this work, we detect methylfluoride molecules by nonresonant multiphoton ionization using a femtosecond laser. Subsequent mass and velocity selection of the produced ions enables us to eliminate most background signal resulting from thermal gas in our vacuum chamber. This detection scheme can be applied to virtually any molecule, thereby greatly enhancing the scope of molecules that can be Stark decelerated. Furthermore, the well-defined detection volume

allows an accurate determination of the density of trapped molecules.

## II. STARK SHIFT OF METHYLFLUORIDE MOLECULES

Methylfluoride,  $\text{CH}_3\text{F}$ , schematically depicted in the right-hand side of Fig. 1, is a prototypical symmetric top molecule. The barrier for inversion in  $\text{CH}_3\text{F}$  is very large; hence, the inversion splitting is predicted to be much smaller than the hyperfine splittings [17]. Consequently, hyperfine levels with opposite parity are completely mixed in electric fields as small as 1 V/cm [11], resulting in a linear Stark shift. In a supersonic expansion, molecules are adiabatically cooled, and only the lowest rotational levels in the vibrational and electronic ground state are populated. In this cooling process, the symmetry of the nuclear spin wave function is preserved. Therefore, the ratio of ortho- to para-methylfluoride is the same in the beam as it is in the reservoir. Figure 1 shows the distribution over different rotational levels in a molecular beam with a temperature of 5 K as a function of the Stark shift at 90 kV/cm (the maximum electric field on the molecular beam axis in our Stark decelerator). For the settings used in our experiment, molecules in states that have a Stark shift larger than  $0.8 \text{ cm}^{-1}$  at 90 kV/cm are decelerated in a phase-stable fashion. This implies that only molecules in the  $|J, MK\rangle = |1, -1\rangle$  state, the ground state of para-methylfluoride that is populated by 11% of the beam, are decelerated.

## III. EXPERIMENTAL SETUP

The experiments described in this paper are performed in a vertical molecular beam machine that was used earlier to decelerate and trap ammonia molecules [10,19,20]. A mixture of 5% methylfluoride molecules in xenon is released into vacuum using a pulsed valve (General Valve Series 9) that is cooled to 173 K, resulting in a beam with an average velocity of around 315 m/s and a velocity spread of 60 m/s. Methylfluoride molecules in the  $|J, MK\rangle = |1, -1\rangle$  state are decelerated to 90–150 m/s using a conventional Stark decelerator consisting of 101 pairs of electrodes to which voltages of +10 kV and –10 kV are applied. The traveling-wave decelerator, which is mounted 24 mm above the last electrode pair of the first decelerator, consists of a series

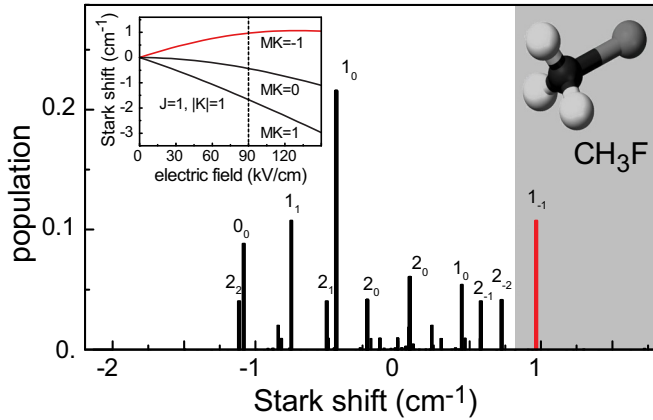


FIG. 1. (Color online) Distribution of  $\text{CH}_3\text{F}$  molecules over different Stark states in a molecular beam with a rotational temperature of 5 K. The Stark shift at 90 kV/cm is calculated using the molecular constants given by Papoušek *et al.* [18]. Levels are (nonuniquely) labeled by  $J_{MK}$ . The inset shows the Stark shift of the  $J = 1, |K| = 1$  state as a function of the applied electric field.

of 336 rings, each of which is attached to one of eight stainless steel rods to which voltages of up to  $\pm 5$  kV are applied. At any moment in time, the voltages applied to successive ring electrodes follow a sinusoidal pattern in  $z$ , where  $z$  is the position along the beam axis. These voltages create minima of electric field every 6 mm that act as three-dimensional (3D) traps for weak-field-seeking molecules. By modulating the voltages sinusoidally in time, the traps are moved along the decelerator; a constant modulation frequency results in a trap that moves with a constant positive velocity along the molecular beam axis, while a constant acceleration can be achieved by applying a linear chirp to the frequency [8,9].

The molecules are ionized 20 mm above the traveling-wave decelerator using pulses of light from a commercial laser system consisting of a titanium:sapphire oscillator (Spectra-Physics, Tsunami) and a chirped regenerative amplifier (Spectra-Physics, Spitfire Pro). Using a 300-mm lens, the fundamental laser output at 800 nm (2 mJ per pulse,  $\tau = 150$  fs) is focused to a  $(1/e)$  spot size of  $25 \times 15 \mu\text{m}^2$ , giving a peak intensity of above  $10^{14}$  W/cm<sup>2</sup>. This intensity is sufficient to ionize virtually any molecule in the laser focus. Using an ion lens, the produced ions are focused onto a double microchannel plate (MCP) mounted in front of a fast response ( $1/e$  time  $\sim 10$  ns) phosphor screen (Photonis P-47 MgO). The light of the phosphor screen is imaged onto a CCD camera and monitored by a photomultiplier tube (PMT). By applying voltages of 2 and 1.1 kV to the first and second extraction plate, respectively, ions with the same initial velocity are focused at the same position on the detector (velocity map imaging (VMI) [21]). A mask on the back side of the phosphor screen is used to pass light from the central part of the image onto a photomultiplier only, thereby collecting light originating from molecules with a small transverse velocity [22]. In this way we can discriminate signal from the (decelerated) beam from signal originating from thermal gas in the chamber [23]. The signal from the PMT is digitized and ions with an arrival time that corresponds to mass 34 ( $\text{CH}_3\text{F}^+$ ) and 15 ( $\text{CH}_3^+$ ) are monitored.

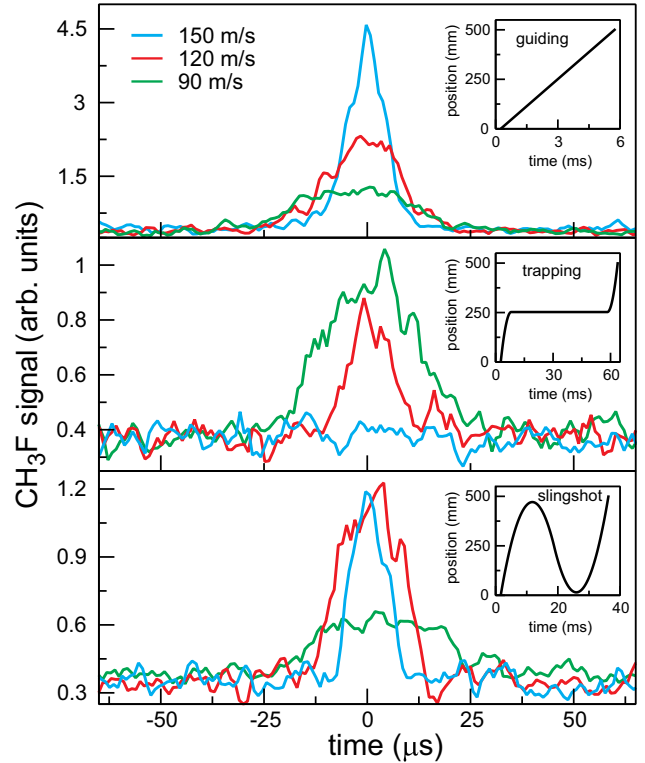


FIG. 2. (Color online) Observed TOF profiles for methylfluoride when waveforms are applied to the traveling-wave decelerator to guide the molecules at a constant speed (top panel), to bring the decelerator to a standstill in the middle of the decelerator, to trap the molecules for 50 ms and accelerate them to their initial velocity (middle panel), and to bring the molecules to a standstill near the end of the traveling-wave decelerator, move them back to the beginning of the decelerator, and accelerate them to their original velocity (bottom panel). The inset shows the position of the electric field minimum with respect to the beginning of the traveling-wave decelerator as a function of time for molecules that are decelerated to 90 m/s.

#### IV. DECELERATING AND TRAPPING METHYLFLUORIDE MOLECULES

Figure 2 shows experimental time-of-flight (TOF) profiles for decelerated methylfluoride molecules when different waveforms are applied to the traveling-wave decelerator. The position of the electric field minimum with respect to the beginning of the traveling-wave decelerator as a function of time is shown in the inset. The horizontal axis is always centered around the expected arrival time of the molecules. The blue, red, and green curves correspond to the situation where molecules are decelerated using the conventional Stark decelerator from 282 to 150 m/s, 266 to 120 m/s, and 257 to 90 m/s, respectively. For the measurements shown in the upper graph, the traveling-wave decelerator is used to guide the molecules at a constant speed. The observed decrease in signal from 150 to 90 m/s is mainly attributed to the lower intensity at the starting velocity in the Stark decelerator.

The middle panel of Fig. 2 shows similar measurements when waveforms are applied to the traveling-wave decelerator that decelerate molecules with a rate of  $48 \times 10^3$ ,  $30 \times 10^3$ , and  $17 \times 10^3$  m/s<sup>2</sup>, respectively, bring them to a standstill

in the middle of the decelerator, trap them for 50 ms, and subsequently accelerate them to their original velocity with an opposite acceleration. The signal for trapped molecules starting from 90 m/s is virtually the same as that of guided molecules at this velocity, which again demonstrates that, at a sufficiently low acceleration, a traveling-wave decelerator can decelerate and trap molecules without losses [20]. For 120 m/s the required acceleration is close to the maximal acceleration that can be exerted on methylfluoride molecules in our decelerator and the trapped signal is about a factor of 2 smaller than that of the guided molecules. For 150 m/s no trapped signal is observed.

The bottom panel of Fig. 2 shows measurements when a waveform is applied to bring methylfluoride molecules to a standstill near the end of the traveling-wave decelerator, move them back to the beginning of the decelerator, and accelerate them to their original velocity. Effectively, this doubles the length of the decelerator and halves the required acceleration, thus making it possible to trap molecules that are injected with a large velocity. As observed, however, the slingshot sequence introduces some additional losses. For molecules that are injected with 90 m/s, the intensity of molecules that were decelerated with the “slingshot” waveform is 50% smaller than the guided or trapped molecules. For molecules that are injected with 120 m/s the intensity is 55% smaller than the guided molecules, but twofold larger than the trapped signal. For molecules that are injected with 150 m/s the intensity is fivefold smaller than the guided molecules [24].

## V. TEMPERATURE AND DENSITY OF TRAPPED METHYLFLUORIDE MOLECULES

We determine the temperature of the trapped molecules by lowering the depth of the trap and monitor which fraction of the molecules remains. If the temperature of the cloud is much lower than the trap depth, the voltages can be lowered without substantial losses. If, on the other hand, the temperature of the cloud is essentially the same as the trap depth, a large loss will occur when the voltages are lowered only slightly. Note that if the voltages are lowered slowly, the molecules are also cooled adiabatically; the velocity spread of the trapped molecules is lowered at the expense of an increased position spread [10,19,20]. Figure 3(a) shows the result of such an experiment. The solid lines denote results from simulations assuming (initial) temperatures of 30, 40, and 60 mK. From this we conclude that the temperature of the trapped methylfluoride molecules is around 40 mK.

In order to translate the number of detected ions into the density and the total number of trapped methylfluoride molecules, we need to know the detection volume. For a highly nonlinear process this turns out to be remarkably simple. As at least eight photons are required to ionize methylfluoride, we expect that if the laser light is of low intensity the ion signal scales with the eighth power of the intensity. At higher intensities, however, virtually all molecules within a certain distance from the laser focus will be ionized. If the laser intensity is increased further, the increase in signal only reflects the increase of the detection volume. For a laser beam with a Gaussian intensity profile of peak intensity  $I_0$  and intensity

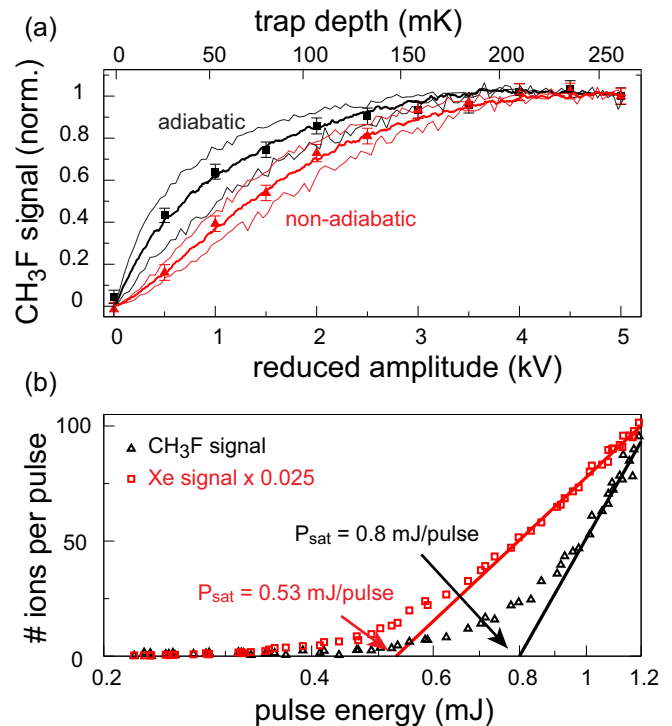


FIG. 3. (Color online) (a) Trapped methylfluoride signal (background subtracted) as a function of the amplitude of the waveform when the trap is slowly (squares) or abruptly (triangles) reduced. The solid lines are simulations that assume an initial temperature of 30, 40, and 60 mK. (b) Ion signal for methylfluoride (sum of  $\text{CH}_3\text{F}^+$  and  $\text{CH}_3^+$ ) and xenon (sum of  $\text{Xe}^+$ ,  $\text{Xe}^{2+}$ , and  $\text{Xe}^{3+}$ ) as a function of the pulse energy. The solid lines show fits to the data assuming a sudden-onset model.

$I_0/e$  at radius  $R$ , the ion signal becomes equal to [25]

$$S = \alpha c l \pi R^2 \ln(I_0/I_{\text{sat}}) \quad (1)$$

with  $\alpha$  the detector efficiency,  $c$  the density of molecules,  $l$  the length over which ions are collected along the direction of laser propagation, and  $I_{\text{sat}}$  a characteristic intensity that indicates the relative ease of ionization for a certain molecule.

Figure 3(b) shows the ion signal for methylfluoride and xenon recorded in the undecelerated molecular beam as a function of the pulse energy. The solid lines show fits to the data using Eq. (1), where the peak intensity  $I_0$  is related to the pulse energy  $P$  via  $I_0 \approx P/\pi R^2 \tau$ , with  $\tau$  the pulse duration. By scaling our data to the saturation intensity for xenon,  $I_{\text{sat}} = 63 \text{ TW/cm}^2$  [26], we find a beam radius  $R = 41 \mu\text{m}$ . This is somewhat larger than the one inferred from measurements of the spatial extent of the beam at the lens, which is attributed to the fact that the spatial profile of our laser beam is not perfectly Gaussian. The saturation intensity of CH<sub>3</sub>F is then found to be  $95 \text{ TW/cm}^2$ , in reasonable agreement with Tanaka *et al.* [27]. Taking the efficiency of our MCP detector,  $\alpha$ , to be 0.6 [28] and  $l$  to be 2.8 mm, we finally find the CH<sub>3</sub>F density in the beam to be  $2.6 \times 10^7 \text{ cm}^{-3}$ , and the xenon density to be  $5.5 \times 10^8 \text{ cm}^{-3}$ . Typically, the signal for trapped CH<sub>3</sub>F molecules is  $\sim 14$  times less than that of the beam. Taking into account that the cloud expands slightly from the decelerator to the detection region, this implies that

our trap contains about  $2 \times 10^4$  molecules at a peak density of  $4.5 \times 10^7 \text{ cm}^{-3}$ .

## VI. CONCLUSION

In conclusion, we have decelerated and trapped methylfluoride ( $\text{CH}_3\text{F}$ ) molecules using a combination of a Stark decelerator and a traveling-wave decelerator. Because of its favorable ratio of Stark shift to mass, methylfluoride is an ideal candidate for Stark-deceleration experiments [3,29]. Here, we detect methylfluoride molecules by nonresonant multiphoton ionization using a femtosecond laser. This detection method can be applied to virtually any molecule, thereby enhancing the scope of molecules that can be Stark decelerated. Furthermore, we show that this detection scheme can be used to accurately determine the density of trapped molecules. A disadvantage of nonresonant multiphoton ionization is that it is not state selective; however, we show that rotational cooling in the supersonic expansion combined with state selection in the Stark decelerator

provides us with a pure sample of para-methylfluoride in the rotational ground state. Furthermore, we show that by using velocity map imaging and mass selection we can suppress signals from thermal gas in our chamber. With a more elaborate VMI setup, the background can be suppressed further. Methylfluoride is so far the heaviest and most complex molecule that has been decelerated to rest. By increasing the length of the traveling-wave decelerator [30] or starting from a buffer gas beam [31,32], even heavier molecules could be trapped, opening up the study of cold large polyatomic molecules.

## ACKNOWLEDGMENTS

This research has been supported by the FOM program “Broken Mirrors & Drifting Constants.” C.M. gratefully acknowledges financial support from the China Scholarship Council. We acknowledge the expert technical assistance of Rob Kortekaas. We thank Paul Jansen, Maurice Janssen, Jaap Bulthuis, Steven Stolte, and Wim Ubachs for useful discussions and support.

- 
- [1] L. D. Carr, D. DeMille, R. V. Krems, and J. Ye, *New J. Phys.* **11**, 055049 (2009).
- [2] S. D. Hogan, M. Motsch, and F. Merkt, *Phys. Chem. Chem. Phys.* **13**, 18705 (2011).
- [3] S. Y. T. van de Meerakker, H. L. Bethlem, N. Vanhaecke, and G. Meijer, *Chem. Rev.* **112**, 4828 (2012).
- [4] E. Narevicius and M. G. Raizen, *Chem. Rev.* **112**, 4879 (2012).
- [5] H. L. Bethlem, G. Berden, A. J. A. van Rooij, F. M. H. Crompvoets, and G. Meijer, *Phys. Rev. Lett.* **84**, 5744 (2000).
- [6] S. Y. T. van de Meerakker, N. Vanhaecke, H. L. Bethlem, and G. Meijer, *Phys. Rev. A* **71**, 053409 (2005).
- [7] S. Y. T. van de Meerakker, N. Vanhaecke, H. L. Bethlem, and G. Meijer, *Phys. Rev. A* **73**, 023401 (2006).
- [8] A. Osterwalder, S. A. Meek, G. Hammer, H. Haak, and G. Meijer, *Phys. Rev. A* **81**, 051401 (2010).
- [9] S. A. Meek, M. F. Parsons, G. Heyne, V. Platschkowski, H. Haak, G. Meijer, and A. Osterwalder, *Rev. Sci. Instrum.* **82**, 093108 (2011).
- [10] M. Quintero-Pérez, P. Jansen, T. E. Wall, J. E. van den Berg, S. Hoekstra, and H. L. Bethlem, *Phys. Rev. Lett.* **110**, 133003 (2013).
- [11] J. Bulthuis, J. B. Milan, M. H. M. Janssen, and S. Stolte, *J. Chem. Phys.* **94**, 7181 (1991).
- [12] M. H. M. Janssen, D. H. Parker, and S. Stolte, *J. Chem. Phys.* **100**, 16066 (1996).
- [13] B. Nagels, M. Schuurman, P. L. Chapovsky, and L. J. F. Hermans, *Phys. Rev. A* **54**, 2050 (1996).
- [14] I. L. Chuang, L. M. Vandersypen, X. Zhou, D. W. Leung, and S. Lloyd, *Nature (London)* **393**, 143 (1998).
- [15] M. L. Wall, K. Maeda, and L. D. Carr, *Ann. Phys.* **525**, 845 (2013).
- [16] M. Zeppenfeld, B. G. U. Englert, R. Glockner, A. Prehn, M. Mielenz, C. Sommer, L. D. van Buuren, M. Motsch, and G. Rempe, *Nature (London)* **491**, 570 (2012).
- [17] S. Wofsy, J. Muentzer, and W. Klemperer, *J. Chem. Phys.* **55**, 2014 (1971).
- [18] D. Papousek, Y.-C. Hsu, H.-S. Chen, P. Pracna, S. Klee, and M. Winnewisser, *J. Mol. Spectrosc.* **159**, 33 (1993).
- [19] P. Jansen, M. Quintero-Pérez, T. E. Wall, J. E. van den Berg, S. Hoekstra, and H. L. Bethlem, *Phys. Rev. A* **88**, 043424 (2013).
- [20] M. Quintero-Pérez, T. E. Wall, S. Hoekstra, and H. L. Bethlem, *J. Mol. Spectrosc.* **300**, 112 (2014).
- [21] A. T. J. B. Eppink and D. H. Parker, *Rev. Sci. Instrum.* **68**, 3477 (1997).
- [22] M. H. M. Janssen, D. H. Parker, G. O. Sitz, S. Stolte, and D. W. Chandler, *J. Phys. Chem.* **95**, 8007 (1991).
- [23] M. Quintero-Pérez, P. Jansen, and H. L. Bethlem, *Phys. Chem. Chem. Phys.* **14**, 9630 (2012).
- [24] Although methylfluoride molecules in the  $J = 1, MK = -1$  state are strongly oriented ( $P_1 = 0.5$ ) and modestly aligned ( $P_2 \sim 0.1$ ) by the electric field used to extract the ions, we did not observe a dependence of the ion signal on the polarization of the laser beam.
- [25] S. M. Hankin, D. M. Villeneuve, P. B. Corkum, and D. M. Rayner, *Phys. Rev. A* **64**, 013405 (2001).
- [26] M. Lezius, V. Blanchet, M. Y. Ivanov, and A. Stolow, *J. Chem. Phys.* **117**, 1571 (2002).
- [27] M. Tanaka, M. Murakami, T. Yatsushashi, and N. Nakashima, *J. Chem. Phys.* **127**, 104314 (2007).
- [28] G. Fraser, *Int. J. Mass Spectrom.* **215**, 13 (2002).
- [29] D. Lian-Zhong, F. Guang-Bin, and Y. Jian-Ping, *Chin. Phys. B* **18**, 149 (2009).
- [30] J. E. van den Berg, S. C. Mathavan, C. Meinema, J. Nauta, T. H. Nijbroek, K. Jungmann, H. L. Bethlem, and S. Hoekstra, *J. Mol. Spectrosc.* **300**, 22 (2014).
- [31] N. E. Bulleid, R. J. Hendricks, E. A. Hinds, S. A. Meek, G. Meijer, A. Osterwalder, and M. R. Tarbutt, *Phys. Rev. A* **86**, 021404 (2012).
- [32] N. R. Hutzler, H.-I. Lu, and J. M. Doyle, *Chem. Rev.* **112**, 4803 (2012).